JACS
JOURNAL OF THE AMERICAN CHEMICAL SOCIETY
Communication
pubs.acs.org/JACS

Facile "Modular Assembly" for Fast Construction of a Highly Oriented Crystalline MOF Nanofilm

Gang Xu,[†] Teppei Yamada,[†] Kazuya Otsubo,[†,‡] Shun Sakaida,[†] and Hiroshi Kitagawa*[,†,‡,§,∥]

[†]Division of Chemistry, Graduate School of Science, Kyoto University, Kitashirakawa Oiwake-cho, Sakyo-ku, Kyoto 606-8502, Japan
[‡]Core Research for Evolutional Science and Technology (CREST), Japan Science and Technology Agency (JST), 5 Sanban-cho, Chiyoda-ku, Tokyo 102-0075, Japan
[§]Institute for Integrated Cell-Material Sciences (iCeMS), Kyoto University, Yoshida, Sakyo-ku, Kyoto 606-8501, Japan
[∥]INAMORI Frontier Research Center, Kyushu University, 744 Motooka, Nishi-ku, Fukuoka 819-3095, Japan

Supporting Information

ABSTRACT: The preparation of crystalline, ordered thin films of metal−organic frameworks (MOFs) will be a critical process for MOF-based nanodevices in the future. MOF thin films with perfect orientation and excellent crystallinity were formed with novel nanosheet-structured components, Cu−TCPP [TCPP = 5,10,15,20-tetrakis(4-carboxyphenyl)porphyrin], by a new "modular assembly" strategy. The modular assembly process involves two steps: a "modularization" step is used to synthesize highly crystalline "modules" with a nanosized structure that can be conveniently assembled into a thin film in the following "assembly" step. With this method, MOF thin films can easily be set up on different substrates at very high speed with controllable thickness. This new approach also enabled us to prepare highly oriented crystalline thin films of MOFs that cannot be prepared in thin-film form by traditional techniques.

Metal−organic frameworks (MOFs), or porous coordination polymers (PCPs), are a class of crystalline hybrid materials formed by the connection of metal centers or clusters and organic linkers. The large surface area, ordered crystalline structure, and highly regularized pores of MOFs produce their popular properties, such as gas storage, separations, sensors, catalysis, and drug delivery.[1] MOFs also have potential for application in fuel cells, solar cells, and nanotechnology devices,[2] and some of these applications require the use of this porous material in thin-film form.[3] In the past few years, increasing effort has gone into preparing substrate-supported MOF thin films.[3,4]

Several methods have been developed to fabricate two types of MOF thin films: one type is polycrystalline MOF films, which typically have MOF crystals or particles randomly placed on a substrate with poorly controlled thickness in the micrometer range; the other type, called SURMOFs, consist of surface grown, crystalline, oriented MOF multilayers that are ultrathin, highly oriented, and thickness-adjustable.[4] Obviously, SURMOFs are superior to polycrystalline MOF films in giving better control of the thickness and the arrangement of the porous channels or cavities and therefore are favored materials for applications.[5]

Some MOF materials that can be synthesized under mild conditions have been successfully applied as SURMOFs. However, the preparation of MOF thin films in a highly crystalline state with a perfectly oriented framework and controllable thickness and their convenient characterization using normal lab instruments are still great challenges.[5,6] In this paper, we report a "modular assembly" method for preparing MOF thin films in two steps. In the "modularization" step, any of the methods developed for bulk MOF synthesis, including solvothermal reactions, can be applied to produce highly crystalline MOF "modules". The subsequent "assembly" step involves rapidly mounting the modules on a highly oriented MOF thin film in a simple manner. Notably, the experimental conditions (e.g., temperature, solvents, and environment) in the assembly step can be totally different from those in the modularization step. The advantages of modular assembly include not only the fact that harsh conditions can be introduced into the preparation of MOF thin films and that MOF thin films can be prepared by a much easier process in a shorter period but also that the obtained MOF thin films would show almost the same traits as a SURMOF, such as crystalline state, oriented framework, and controllable growth from the substrate. In this work, high-aspect-ratio nanosheet-structured MOFs, Cu−TCPP, were synthesized as modules that then were assembled via a simple and fast "stamping" process to form thin films on various substrates. The modules were synthesized using a solvothermal reaction, while the thin films were assembled under ambient conditions. Here we first report this facile modular assembly method for constructing highly oriented crystalline MOF thin films using a very convenient and fast process.

Novel Cu−TCPP nanosheets were synthesized by the solvothermal reaction of $Cu(NO_3)_2{\cdot}3H_2O$ and 5,10,15,20-tetrakis(4-carboxyphenyl)porphyrin (H_2TCPP) in a mixture of *N*,*N*-diethylformamide and ethanol [for details, see the Supporting Information (SI)]. The scanning electron microscopy (SEM) image showed that the as-synthesized particles formed a collection of flakes with a high aspect ratio (Figure S1a in the SI). The flaky sample was able to be dispersed in ethanol or acetone very well by ultrasonication and formed a

Received: August 9, 2012
Published: October 2, 2012

dx.doi.org/10.1021/ja307953m | J. Am. Chem. Soc. 2012, 134, 16524−16527

purple colloidal suspension. The Tyndall effect (Figure S2) confirmed the fine dispersion of the nanosheets in the suspension. The dispersion was used to prepare the samples for transmission electron microscopy (TEM) and atomic force microscopy (AFM). As shown in the TEM images (Figure 1a,b), the nanosheets had a very smooth surface and diameters

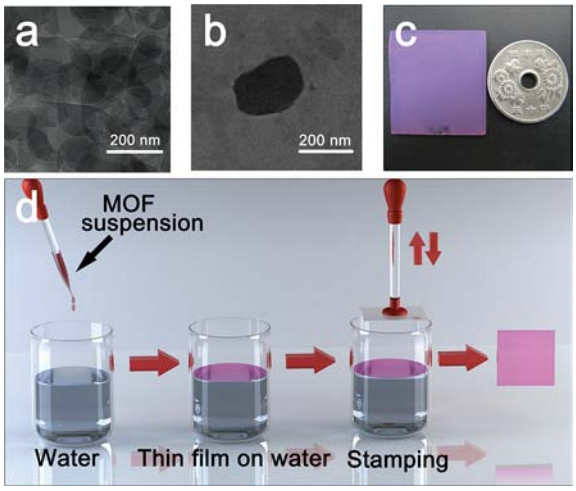

Figure 1. (a, b) TEM images of the synthesized Cu−TCPP nanosheets. (c) Photograph of the MOF thin film after 15 deposition cycles on a quartz substrate. (d) Illustration of the assembly process of this MOF thin film.

of 300−500 nm. The uniform contrast in the TEM image suggests a uniform thickness of the nanosheets, while the darker area is due to the overlapped assembly of neighboring nanosheets. AFM measurements of individual nanosheets confirmed the value for the diameter and also showed that these nanosheets had a very uniform thickness of ∼15 nm (Figure S1b).

After being dispersed in solvents by ultrasonication, these nanosheets did not show any curling (Figure 1a). This type of flat and high-aspect-ratio nanosheet is very desirable because of its advantages over isotropic nanoparticles in regard to packing and processing to produce a highly oriented and packed membrane.[7] Following the modular assembly concept, the crystalline Cu−TCPP nanosheets were suitable modules for assembly into a MOF thin film by a simple stamping process. As shown in Figure 1d, the modular assembly was conducted as follows: first, the as-synthesized nanosheets were dispersed in ethanol by ultrasonication to obtain a purple colloidal suspension with a typical concentration of 1.0 mg cm^{-3}; second, the suspension was placed dropwise onto the surface of water in a beaker, which served as a perfectly flat substrate, and because of the hydrophobic property of the Cu−TCPP nanosheets, they spontaneously spread out to form a thin film (see the movie in the SI); finally, the thin film was easily transferred to a solid substrate (e.g., a Au/Si wafer or quartz plate) by stamping. After the film was immersed in pure water in another beaker to remove undeposited nanosheets and the small amount of water on the substrate was blown away, additional nanosheets could be repeatedly stacked in a layer-by-layer (LBL) growth model to create a MOF thin film with the desired thickness.

The growth of a MOF thin film on a quartz substrate was monitored by UV−vis absorption spectroscopy. Figure 2 shows successful LBL film deposition with linear growth, demonstrat-

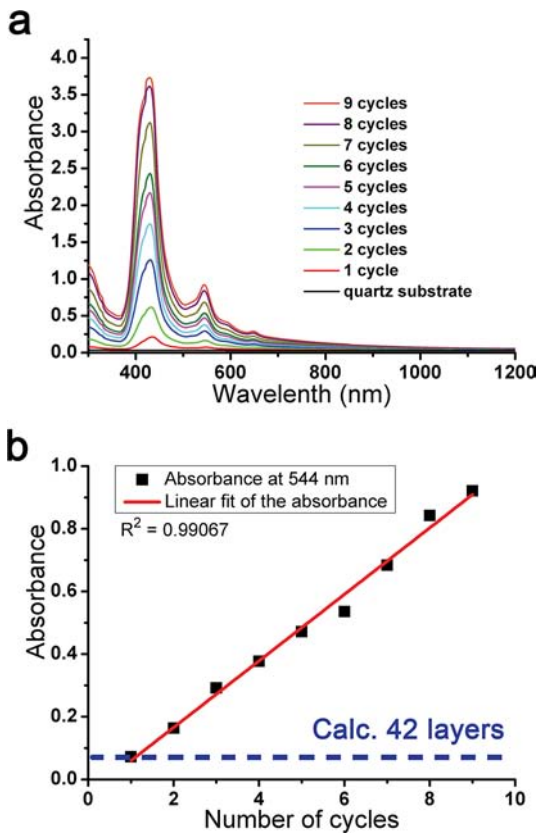

Figure 2. (a) LBL assembly of a thin film observed by UV−vis absorption. (b) Plot of the maximum absorbance of Cu−TCPP at 544 nm vs the number of film-growth cycles.

ing that each stacking cycle resulted in deposition of the same amount of material. By calculation from the absorbance, one deposition cycle grew an average of 42 layers of porphyrin molecules. Since the average thickness of the Cu−TCPP nanosheets was 15 nm, corresponding to 33 layers of porphyrin molecules in the unit cell of the modeled crystal structure below, one deposition cycle stacked ∼1.3 layers of nanosheets on average. Compared with the traditional method for preparing MOF thin films, our modular assembly protocol achieved a higher deposition speed, as more than 100 layers could be grown within 10 min. Figure 1c shows a homogeneous thin film after 15 deposition cycles on a quartz substrate using this stamping method.

The modular assembly protocol endowed the prepared MOF thin film with relatively thick and highly crystalline modules with a huge domain size of up to several hundred nanometers. This enabled us to obtain high-quality X-ray diffraction (XRD) patterns. XRD measurements on the MOF thin film (20 deposition cycles) on a Au/Si substrate were accomplished using laboratory equipment (Cu Kα), and intense peaks were observed with a short exposure time of only 20 s/step, compared with the 1000 s/step for traditional LBL liquid-phase epitaxy (Figure 3).[5,6] The clearly distinguishable diffraction pattern shows the high crystallinity of the thin film. The XRD patterns were collected using two different scattering geometries: out-of-plane and in-plane.[3] Figure 3a shows the in-plane profile of the thin film measured using grazing-incidence XRD (GIXRD) technique at an incident angle (α) of 0.2°. The prepared thin film was synthesized with starting materials quite similar to those for NAFS-1 and NAFS-2 in our previous work

dx.doi.org/10.1021/ja307953m | J. Am. Chem. Soc. 2012, 134, 16524−16527

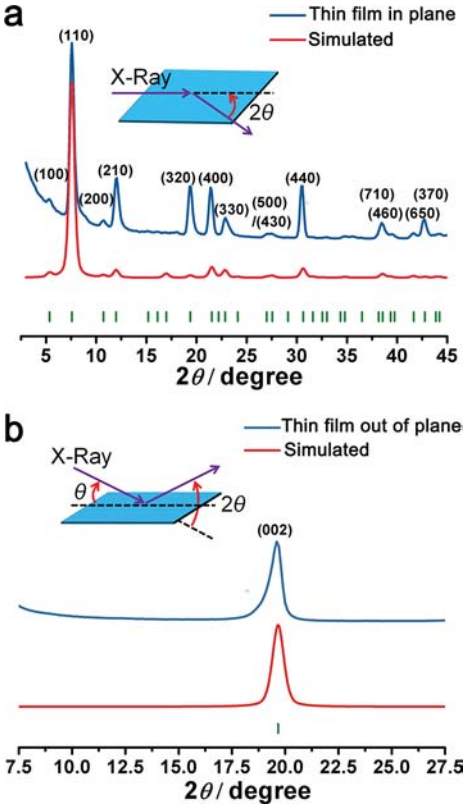

Figure 3. Observed and simulated (a) in-plane and (b) out-of-plane XRD profiles of the prepared MOF thin film. The simulated profiles were obtained using the suggested structural model depicted in Figure 4.

and has very similar diffraction profiles,[3] indicating that they should have comparable crystal structures. On the basis of the results for NAFS-1 and NAFS-2, we modeled a possible crystal structure on a tetragonal unit cell for the thin film in this work (Figure 4). The dimension of *a* in the unit cell, 1.6496 nm as

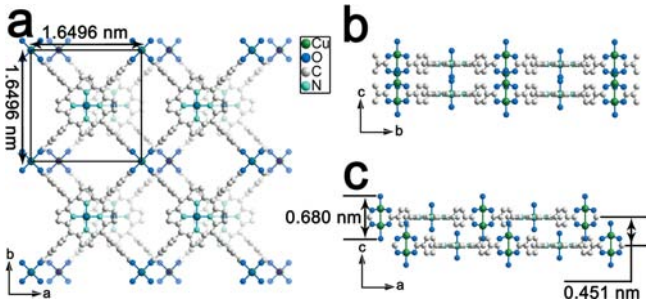

Figure 4. Projections of the proposed crystal structure of the MOF thin film on the (a) *ab* plane, (b) *bc* plane, and (c) *ac* plane. H atoms have been omitted for clarity.

calculated from the in-plane XRD profile, is similar to those in NAFS-1 and NAFS-2. The lattice parameters and the UV–vis absorption and IR spectra (Figures S3 and S4) are in agreement with a two-dimensional (2D) "checkerboard" structure consisting of Cu-centered TCPP units connected by binuclear $Cu_2(COO)_4$ paddlewheels along the *ab* plane (Figure 4a).[3,8] Along the *c* axis, two "checkerboard" layers (denoted as A and B layers) are packed within the lattice, with the B layers shifted from the vertical positions of the A layers by one-fourth of the unit cell along the *a* axis (Figure 4). The out-of-plane XRD pattern was measured with θ–2θ scans, and a unique peak at ~19.6° was observed and assigned to (002) (Figure 3b). According to Bragg's law, the value of *c* in the crystal lattice was 0.9020 nm, which is double the vertical distance between two neighboring porphyrin layers along the *c* axis (Figure 4b,c). This crystal structure model supports the 2D flake morphology of the Cu–TCPP nanosheets very well. The coordination bonds between the Cu atom and the carboxyl group in the *ab* plane are much stronger than the interactions (e.g., hydrogen-bonding and van der Waals interactions) between the checkerboard layers, which would induce faster growth in the *ab* plane than along the *c* axis during the crystallization process. Because of the inherited relationship between the prepared MOF thin film and the Cu–TCPP nanosheets, the domain size of the MOF thin film as shown by the TEM and AFM images was estimated to be hundreds of nanometers in diameter and ~15 nm in thickness (Figure S1), which are significantly larger than those of previously reported SURMOFs.[3,5] This shows that we can obtain a highly crystalline MOF thin film by this simple modular assembly method.

All of the peaks in the in-plane diffraction could be assigned to (*hk*0), and the peak in the out-of-plane pattern could be assigned to (00*l*). These observations show that the MOF thin film has not only highly crystalline order inside each module but also perfect orientation in the deposition process. The simulated in-plane GIXRD pattern with AB layer packing agrees very well with our experiment. On the other hand, the simulated pattern obtained assuming AA layer packing shows poorer agreement with the experimental results (Figure S5).

More details of the structural information on the prepared thin film were obtained by the rocking curve (θ scan) and azimuthal angle dependence (Φ scan) measurements at the (002) position (Figure S6). In Figure S6a, a broad peak in the rocking curve with the top position at 9.2° and a full width at half-maximum of ~7.2° suggested that the average tilting angle between two neighboring stacking layers was ~7.2°. The intensity of the (002) peak presented no azimuthal angle dependence (Figure S6b), showing that the modules were homogeneously mounted on the substrate. This uniform deposition of the thin film can also be clearly observed in the microscopy photos (Figure S7).

In conclusion, we have demonstrated a facile "modular assembly" method that can be used to construct highly oriented crystalline MOF thin films using a very convenient and fast process. With this method, the MOF thin film is fabricated in two steps: In the "modularization" step, the MOF of interest, which can even be a MOF requiring harsh synthesis conditions, is produced as "modules" to be used in the formation of the MOF thin film. The subsequent "assembly" step for growing the thin film endows us with the ability to stack the modules quickly onto MOF thin films. The method was validated by the preparation of a MOF thin film using Cu–TCPP nanosheets as modules and assembling these modules to form MOF thin films via a simple "stamping" process. The prepared MOF thin film possessed almost the same traits as a SURMOF, such as a highly crystalline state, perfectly oriented framework, and controllable thickness, but was obtained with much greater speed and an easier process. However, until an annealing process is developed, this method is limited to nanostructured crystallite sizes. We also note that one of the key factors in applying this method to another MOF is to synthesize the anisotropic nanoparticles with relative MOF material. Recently,

dx.doi.org/10.1021/ja307953m | J. Am. Chem. Soc. 2012, 134, 16524–16527

the preparation of 2D MOF and covalent organic framework (COF) nanostructures by both top-down and bottom-up methods has emerged.[9] Therefore, the thin-film growth strategy presented here could immediately be versatilely applied to other interesting MOFs and COFs. What is more, modular assembly should enable highly oriented hybrid MOF thin films with different types of individual layers possessing different functions, such as separation, condensation, and catalysis, to be simply integrated accordingly to fulfill the requirements for practical applications of MOFs in the future.

■ ASSOCIATED CONTENT

Supporting Information

Experimental details, SEM and AFM images, Tyndall effect, FT-IR and UV−vis absorption spectra, simulated XRD pattern for AA packing, rocking curve and azimuthal angle dependence measurements, microscopy photos, and a movie (QT) showing thin-film formation on a water surface. This material is available free of charge via the Internet at http://pubs.acs.org.

■ AUTHOR INFORMATION

Corresponding Author

kitagawa@kuchem.kyoto-u.ac.jp

Notes

The authors declare no competing financial interest.

■ ACKNOWLEDGMENTS

This work was partially supported by Grants-in-Aid for Scientific Research (20350030 and 23245012) from the Ministry of Education, Culture, Sports, Science and Technology of Japan. G.X. thanks JSPS for a postdoctoral fellowship (P11339).

■ REFERENCES

(1) (a) Chae, H. K.; Siberio-Perez, D. Y.; Kim, J.; Go, Y.; Eddaoudi, M.; Matzger, A. J.; O'Keeffe, M.; Yaghi, O. M. *Nature* **2004**, *427*, 523. (b) Farha, O. K.; Shultz, A. M.; Sarjeant, A. A.; Nguyen, A. T.; Hupp, J. T. *J. Am. Chem. Soc.* **2011**, *133*, 5652. (c) Murray, L. J.; Dincă, M.; Long, J. R. *Chem. Soc. Rev.* **2009**, *38*, 1294. (d) Li, J. R.; Sculley, J.; Zhou, H. C. *Chem. Rev.* **2012**, *112*, 869. (e) Shimomura, S.; Higuchi, M.; Matsuda, R.; Yoneda, K.; Hijikata, Y.; Kubota, Y.; Mita, Y.; Kim, J.; Takata, M.; Kitagawa, S. *Nat. Chem.* **2010**, *2*, 633. (f) Sumida, K.; Rogow, D. L.; Mason, J. A.; McDonald, T. M.; Bloch, E. D.; Herm, Z. R.; Bae, T. H.; Long, J. R. *Chem. Rev.* **2012**, *112*, 724. (g) Férey, G.; Mellot-Draznieks, C.; Serre, C.; Millange, F.; Dutour, J.; Surble, S.; Margiolaki, I. *Science* **2005**, *309*, 2040. (h) Hurd, J. A.; Vaidhyanathan, R.; Thangadurai, V.; Ratcliffe, C. I.; Moudrakovski, I. L.; Shimizu, G. K. H. *Nat. Chem.* **2009**, *1*, 705. (i) Kurmoo, M. *Chem. Soc. Rev.* **2009**, *38*, 1353.

(2) (a) Yaghi, O. M.; O'Keeffe, M.; Ockwig, N. W.; Chae, H. K.; Eddaoudi, M.; Kim, J. *Nature* **2003**, *423*, 705. (b) Férey, G. *Chem. Soc. Rev.* **2008**, *37*, 191. (c) Seo, J. S.; Whang, D.; Lee, H.; Jun, S. I.; Oh, J.; Jeon, Y. J.; Kim, K. *Nature* **2000**, *404*, 982. (d) Kitagawa, S.; Kitaura, R.; Noro, S. *Angew. Chem., Int. Ed.* **2004**, *43*, 2334.

(3) (a) Makiura, R.; Motoyama, S.; Umemura, Y.; Yamanaka, H.; Sakata, O.; Kitagawa, H. *Nat. Mater.* **2010**, *9*, 565. (b) Makiura, R.; Kitagawa, H. *Eur. J. Inorg. Chem.* **2010**, 3715. (c) Motoyama, S.; Makiura, R.; Sakata, O.; Kitagawa, H. *J. Am. Chem. Soc.* **2011**, *133*, 5640. (d) Otsubo, K.; Haraguchi, T.; Sakata, O.; Fujiwara, A.; Kitagawa, H. *J. Am. Chem. Soc.* **2012**, *134*, 9605.

(4) (a) Bétard, A.; Fisher, R. A. *Chem. Rev.* **2012**, *112*, 1055. (b) Shekhah, O.; Liu, J.; Fischer, R. A.; Wöll, C. *Chem. Soc. Rev.* **2011**, *40*, 1081. (c) Zacher, D.; Shekhah, O.; Wöll, C.; Fischer, R. A. *Chem. Soc. Rev.* **2009**, *38*, 1418. (d) Tsotsalas, M.; Umemura, A.; Kim, F.; Sakata, Y.; Reboul, J.; Kitagawa, S.; Furukawa, S. *J. Mater. Chem.* **2012**, *22*, 10159. (e) Biemmi, E.; Scherb, C.; Bein, T. *J. Am. Chem. Soc.* **2007**, *129*, 8054. (f) Guo, H.; Zhu, G.; Hewitt, I. J.; Qiu, S. *J. Am. Chem. Soc.* **2009**, *131*, 1646. (g) Ameloot, R.; Stappers, L.; Fransaer, J.; Alaerts, L.; Sels, B. F.; De Vos, D. E. *Chem. Mater.* **2009**, *21*, 2580. (h) Allendorf, M. D.; Houk, R. J. T.; Andruszkiewicz, L.; Talin, A. A.; Pikarsky, J.; Choudhury, A.; Gall, K. A.; Hesketh, P. J. *J. Am. Chem. Soc.* **2008**, *130*, 14404. (i) Kreno, L. E.; Hupp, J. T.; Van Duyne, R. P. *Anal. Chem.* **2010**, *82*, 8042. (j) Ameloot, R.; Gobechiya, E.; Uji-i, H.; Martens, J. A.; Hofkens, J.; Alaerts, L.; Sels, B. F.; De Vos, D. E. *Adv. Mater.* **2010**, *22*, 2685. (k) Carbonell, C.; Imaz, I.; Maspoch, D. *J. Am. Chem. Soc.* **2011**, *133*, 2144. (l) Zhuang, J.-L.; Ceglarek, D.; Pethuraj, S.; Terfort, A. *Adv. Funct. Mater.* **2011**, *21*, 1442. (m) Falcaro, P.; Hill, A. J.; Nairn, K. M.; Jasieniak, J.; Mardel, J. I.; Bastow, T. J.; Mayo, S. C.; Gimona, M.; Gomez, D.; Whitfield, H. J.; Riccò, R.; Patelli, A.; Marmiroli, B.; Amenitsch, H.; Colson, T.; Villanova, L.; Buso, D. *Nat. Commun.* **2011**, *2*, 237. (n) Bux, H.; Liang, F.; Li, Y.; Cravillon, J.; Wiebcke, M.; Caro, J. *J. Am. Chem. Soc.* **2009**, *131*, 16000. (o) Venna, S. R.; Carreon, M. A. *J. Am. Chem. Soc.* **2009**, *132*, 76.

(5) (a) Zacher, D.; Yusenko, K.; Bétard, A.; Henke, S.; Molon, M.; Ladnorg, T.; Shekhah, O.; Schüpbach, B.; Arcos, T. D. L.; Krasnopolski, M.; Meilikhov, M.; Winter, J.; Terfort, A.; Wöll, C.; Fischer, R. A. *Chem.—Eur. J.* **2011**, *17*, 1448. (b) Liu, B.; Ma, M.; Zacher, D.; Bétard, A.; Yusenko, K.; Metzler-Nolte, N.; Wöll, C.; Fischer, R. A. *J. Am. Chem. Soc.* **2011**, *133*, 1734.

(6) Shekhah, O.; Hirai, K.; Wang, H.; Uehara, H.; Kondo, M.; Diring, S.; Zacher, D.; Fischer, R. A.; Sakata, O.; Kitagawa, S.; Furukawa, S.; Wöll, C. *Dalton Trans.* **2011**, *40*, 4954.

(7) Varoon, K.; Zhang, X.; Elyassi, B.; Brewer, D. D.; Gettel, M.; Kumar, S.; Lee, J. A.; Maheshwari, S.; Mittal, A.; Sung, C.; Cococcioni, M.; Francis, L. F.; McCormick, A. V.; Mkhoyan, K. A.; Tsapatsis, M. *Science* **2011**, *334*, 72.

(8) (a) Choi, E. Y.; Barron, P. M.; Novotny, R. W.; Son, H. T.; Hu, C.; Choe, W. *Inorg. Chem.* **2009**, *48*, 426. (b) Chung, H.; Barron, P. M.; Novotny, R. W.; Son, H. T.; Hu, C.; Choe, W. *Cryst. Growth Des.* **2009**, *9*, 3327.

(9) (a) Li, Z.; Qiu, L.; Wang, W.; Xu, T.; Wu, Y.; Jiang, X. *Inorg. Chem. Commun.* **2008**, *11*, 1375. (b) Li, P.; Maeda, Y.; Xu, Q. *Chem. Commun.* **2011**, *47*, 8436. (c) Pham, M.; Vuong, G.; Fontaine, F.; Do, T. *Cryst. Growth Des.* **2012**, *12*, 3091. (d) Dienstmaier, J. F.; Gigler, A. M.; Goetz, A. J.; Knochel, P.; Bein, T.; Lyapin, A.; Reichlmaier, S.; Heckl, W. M.; Lackinger, M. *ACS Nano* **2011**, *5*, 9737.